CrossMark

Bearing Abilities and Progressive Damage Analysis of Three Dimensional Four-Directional Braided Composites with Cut-Edge

Bing Lei[1] · Zhenguo Liu[1] · Jixuan Ya[2] · Yibo Wang[1] · Xiaokang Li[1]

Abstract Cut-edge is a kind of damage for the three-dimensional four-directional (3D4d) braided composites which is inevitable because of machining to meet requisite shape and working in the abominable environment. The longitudinal tensile experiment of the 3D4d braided composites with different braiding angles between cut-edge and the ones without cut-edge was conducted. Then representative volume cell (RVC) with interface zones was established to analyze the tensile properties through the fracture and damage mechanics. The periodic boundary conditions under the cut-edge and uncut-edge conditions were imposed to simulate the failure mechanism. Stress-strain distribution and the damage evolution nephogram in cut-edge condition were conducted. Numerical results were coincident with the experimental results. Finally the variation of cut-edge effect with the specimen thickness was simulated by superimposing inner cells. The consequence showed that thickness increase can effectively reduce cut-edge influence on longitudinal strength for 3D4d braided composites. Cut-edge simulation of braided composites has guiding significance on the actual engineering application.

Keywords Cut-edge · 3D4d braided composites · Interface · Numerical results · Inner cells

1 Introduction

Three-dimensional (3D) braided composites had been studied for decades. As a kind of textile composites, 3D braided composites have been attractive for industrial applications because of

---

✉ Zhenguo Liu
liuzg@buaa.edu.cn

[1] School of Aeronautic Science and Engineering, Beihang University (BUAA), Beijing 100191, People's Republic of China

[2] Shanghai Electric Wind Co. Ltd, Shanghai 200241, People's Republic of China

🄰 Springer

their excellent mechanical performances, such as better out-of-plane stiffness, strength and impact resistance compared to the fiber reinforced laminated composites [1–6]. In recent years, 3D braided composites have been broadly used in thermal protection cone, brake block, the hot-end guard tile and rocket engine throat lining. On one hand, the braided integrity structurally will be damaged in poor working circumstance such as mar, abrasion and ablation. On the other hand, some composites configuration have to be incised on purpose of meeting the final product dimension which will destroy structures and demolish the spatial integrity of the fiber architecture in 3D braided composites.

Experimental investigation on the mechanical property of cut-edge was conducted by Macander [7] in 1986. The result showed that cut-edge had great effect on the tensile, compression and flexure stiffness, strength and poisson ratio for 3D braided composites. The average tensile strength of 3D4d braided composites dropped nearly 60 % over the uncut-edge ones. Li [8] carried out a suite of experiments on the mechanical properties of braided composites between cut-edge and uncut-edge in 2006. The experiments in consideration of three different ways of cut-edge and two braiding angles made a deep research on the effect of the cut-edge. The loss of stiffness and strength on width was less than that ones on thickness which can be attributed to more inner cells along width direction than thickness direction in 3D braided composites.

While cut-edge effect on 3D braided composites was merely researched through experimental method. The loss of strength for cut-edge specimens was obtained, but there was no in-depth study on its stress distribution field and failure mechanism. Further researches on the cut-edge effect of different braiding angels and different braiding patterns are needed, whereas relevant experiments will take much time and cost and limited results may be still restricted to promote the analysis of structural mechanics. Simulation analysis can easily control variables and complete some works which cannot be implemented in the actual experiments. So a research on the cut-edge effect of 3D braided composites using simulation method not only reduces the cost but also has guidance for practical engineering application.

Adopting the method of simulation and experiment was efficient to analyze material mechanical properties. Ref. [9] studied free-edge effect on the effective stiffness of single-layer braided composite by this way in which the number of inner cells represented the width of specimen. In recent years, simulation studies on 3D braided composites had been continuously expanding. Researches have been carried out on the micro-structures and predictions of mechanical properties using finite element method (FEM). Li [10] created a RVC of 3D4d braided composites based on the locus of the yarns' movement which was used to predict the tensile modulus under periodic boundary condition. Zhang [11] established three distinct solid structure models of unit-cell located in the interior, surface and corner regions and studied the stiffness for each cell. Researches of damage evolution about 3D braided composites under longitudinal tensile already had a lot which primarily concentrated on integrated braided composites. Fang [12] established a new RVC and used the progressive damage model to predict the modulus, strength and the damage progress of 3D4d braided composites under tensile and compressive load. He investigated the influence of interface damage to the fracture of the 3D4d braided composites under tension load. Zeng [13] predicted the nonlinear response and damage evolution using finite element method. Hu [14] investigated the progressive damage and failure mechanism of three dimensional full five-directional braided composites. In summary, according

to above literature and Refs. [15–19], it should be noticed that simulation method has been developing rapidly, the research of cut-edge effect by simulation method will promote the researchers' understanding and find a way to improve the mechanical performance after trimming.

This paper is aiming at elucidating the influence of cut-edge on the tensile properties of 3D4d braided composites using progressive damage and nonlinear analysis method. Firstly, longitudinal tensile experiment was conducted for cut-edge and uncut-edge specimens with interior braiding angels20˚ and 40˚.The RVC model of 3D4d braided composites with interface was established and periodic boundary conditions in cut-edge and uncut-edge situations were imposed in section 3. The stress-strain curves in cut-edge and uncut-edge conditions and nephogram of the RVE damage evolution were obtained. Numerical results were compared with the experimental data in section 5. The variation of cut-edge effect with thickness was investigate through progressive damage analysis method in section 6. Finally, some valuable conclusions were obtained.

2 Experiment

2.1 Specimens Preparation

Numbers of research works were focused on mechanical properties of 3D braided composites by experiment methods [20–23]. Experimental research can intuitively reflect the destruction form of the material and ultimate bearing capacity, at the same time provide guidance for the simulation analysis. This paper four-step 1×1 braiding procedure was used to fabricate the preforms. The array of yarn carriers was 24×3 for the 3D4d specimens. The T700-12 K carbon fibers from Toray company were used as reinforcement. The TDE-86 epoxy resins were injected into preforms by the resin transfer molding (RTM) process and then consolidated to produce the specimens. The braided angles of the coupons were 20˚ and 40˚.

3D braided composites are made up of three different regions that are interior cell region, surface cell region and corner cell region as shown in Fig. 1. Zhang [10] studied the three cells models in detail which indicated the thickness of interior cell was 2.39 times as much as the surface cell for the 3D4d braided composites. The experiment specimens were fabricated by three rows so that one interior cell and two surface cells existed in the specimens. The portion of the corner cells and surface cells were incised from the coupon to compared with the below

Fig. 1 The constitution of 3D4d braided composites

Corner cell

Surface cell

Interior cell
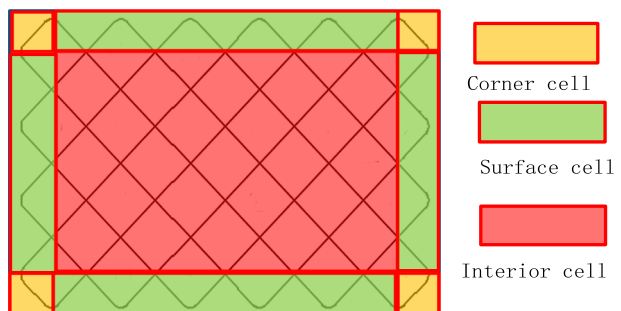
simulation results. Figure 2 showed the cut scheme of 3D4d braided composites. All specimens dimension and the numbers were listed in Table 1.

A series of tensile tests were performed using WDW-2000 testing machine in order to compare the properties and failure mechanisms of 3D braided uncut-edge and cut-edge composites. 3D4dC specimen was shown in Fig. 3.

2.2 Experiment Results

Figure 4 and Fig. 5 showed the damage morphologies of specimens with different braiding angels respectively. The fracture morphologies showing brittle fracture of the 3D4dU specimens were nearly with some yarns fractured. For little braiding angel, there was obviously tensile shear failure of yarns, fiber breakage and no the phenomenon of fiber pulling-out as shown in Fig. 4a. The damage constituent of the 3D4dU braided composites with large braiding angle was controlled by several mechanisms, such as fiber breakage, the localization of matrix cracking and interfacial debonding shown in Fig. 5a. For 3D4dC braided composites, since the breaking yarns in surface destructed the integrity of specimens, the fracture of yarns did not occur while the interface between the fiber bundles damaged. For large braiding angel, interface debonding appeared earlier as there was large shear stress between the fiber bundles and the crack shape of the 3D4dC-40 braided composites liked saw.

3 Finite Element Model

3.1 Geometry Model of RVC

The 3D4d braided composites are fabricated by the 4-step 1 × 1 rectangular braiding method and are made up of four directional braided yarns and resin matrix. Because of the periodic micro-structure of braided composites' structures, the RVC model is used to analyze their
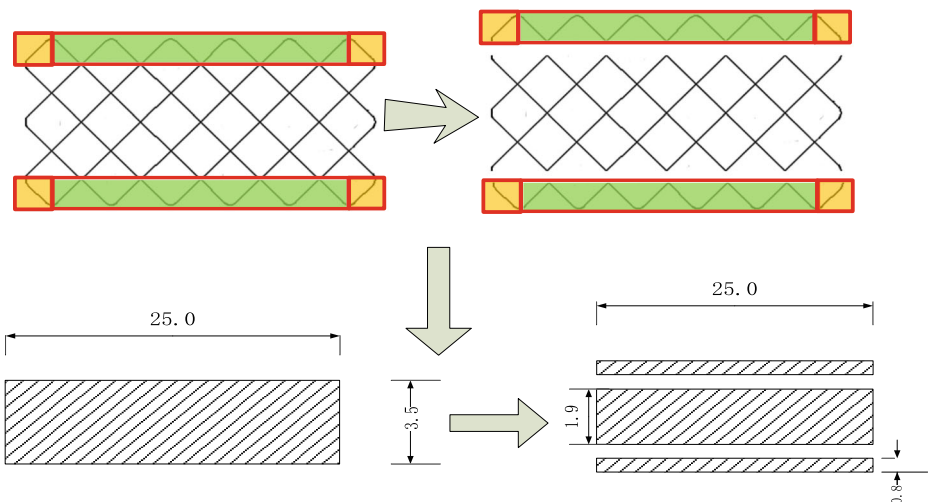

Fig. 2 Cut schematic diagram

Table 1 Numbers and physical dimension of specimens

Specimen number	Braided angle (γ)	Size/mm	Cut-Edge
3D4dU-20	20°	25 × 3.5 × 250	No
3D4dC-20	20°	25 × 1.9 × 250	Yes
3D4dU-40	40°	25 × 3.5 × 250	NO
3D4dC-40	40°	25 × 1.9 × 250	YES

mechanical properties. Some assumptions have been proposed based on the analysis to establish the RVC.

1) The path of yarns in the interior of 3D4d braided composites keeps straight based on simulation of braid process as shown in Fig. 6a.
2) The cross section shape of the braiding yarn is hexagon in Fig. 6b.
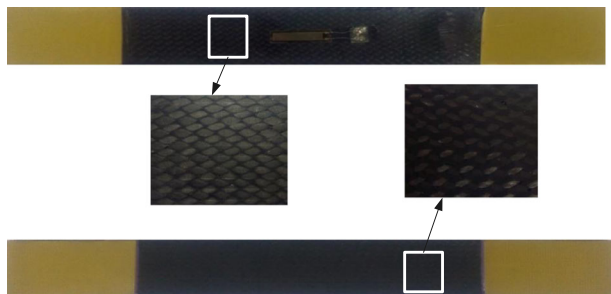3) Every two yarns in the RVC is surface contacted in Fig. 6c.

According to the geometric relationships, the relations of geometry parameters of the RVC can be expressed as follows:

$$a = \phi\sqrt{\frac{2\pi N}{3\cos\gamma\kappa}} \tag{1}$$

$$\begin{cases} c = \dfrac{a}{4}\sqrt{1 + \cos\gamma^2} \\ d = \dfrac{a}{2}\cos\gamma \\ \theta = 2\arcsin\left(\dfrac{1}{\sqrt{1 + \cos\gamma^2}}\right) \end{cases} \tag{2}$$

$$H = \frac{2\phi}{\tan\gamma}\sqrt{\frac{2N\pi}{\cos\gamma\kappa}} \tag{3}$$

Fig. 3 3D4dC specimen

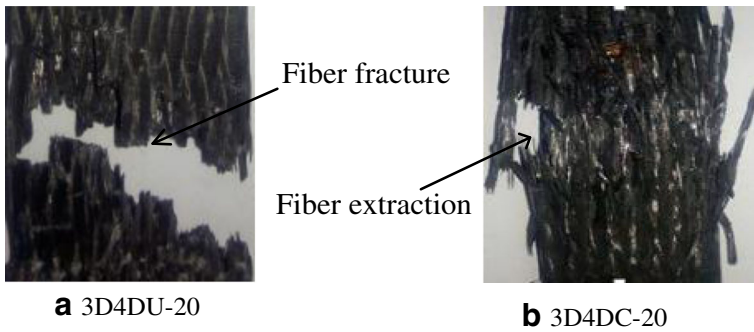**a** 3D4DU-20   **b** 3D4DC-20

Fig. 4 The fracture morphologies of the 3D4d specimens with $\gamma = 20°$

$$W = T = \sqrt{2} \ a \tag{4}$$

H denotes braiding pitch length and the height of RVC. W and T are the width and thickness of RVC respectively. κ is the compact factor of the fiber tow.

Due to the micro-structure complexity, the tetrahedron elements are applied to mesh the braiding yarns and resin. In order to study the effect of the interfaces damage, the interface elements whose behavior is characterized by cohesive model are created. It is assumed that there is a very thin layer of interface which is controlled by a Cohesive Zone Model (CZM) using to predict the interfacial debonding behavior in Refs. [24–26]. A 6-node cohesion element (COH3D6) is implemented in the ABAQUS finite element code.

3.2 Periodical Boundary Condition

The boundary condition is very crucial to predict the mechanical properties by the RVC model, ordinary periodic boundary is imposed to the RVC to keep stress and strain continuous among the three opposite faces in previous study. In this paper, ordinary periodic boundary condition is used to simulate the specimens in the uncut-edge condition according to Eq. 3–5. The experiment specimens are fabricated by three rows of carriers so that one interior cell and two surface cells distribute in the specimens, When the surface cells are removed from the coupon which will lead to no periodicity and only one inner cell in the T-T direction, here T-T direction represents the direction along thickness as shown in Fig. 7. So new periodic boundary condition should be imposed to the other two opposite faces according to Eq.3–6.
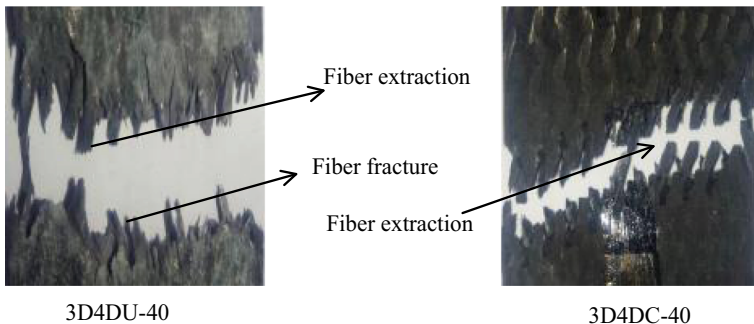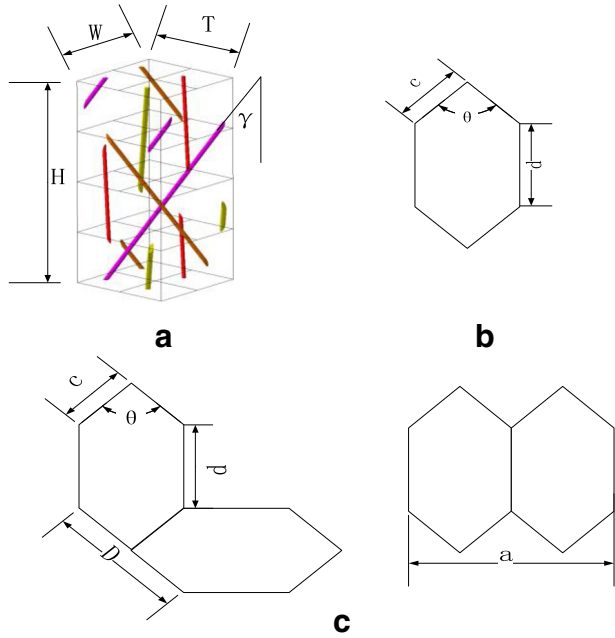

3D4DU-40   3D4DC-40

Fig. 5 The fracture morphologies of the 3D4d specimens with $\gamma = 40°$

Fig. 6 RVC model of 3D4d braided composites. **a** The distributions of yarns; **b** The cross section of braiding yarns; **c** Contacting relation of braiding yarns

$$\begin{cases} U_{\text{BCGF}} - U_{\text{ADHE}} = U_B - U_A = U_B, V_{\text{BCGF}} - V_{\text{ADHE}} = 0, W_{\text{BCGF}} - W_{\text{ADHE}} = 0 \\ W_{\text{EFGH}} - W_{\text{ABCD}} = W_E - W_A = W_E, U_{\text{EFGH}} - U_{\text{ABCD}} = 0, V_{\text{EFGH}} - V_{\text{ABCD}} = 0 \\ V_{\text{CDHG}} - V_{\text{ABEF}} = U_D - U_A = U_D, U_{\text{CDHG}} - U_{\text{ABEF}} = 0, W_{\text{CDHG}} - W_{\text{ABEF}} = 0 \\ U_A = V_A = W_A = 0, W_B = U_D = V_E = 0 \end{cases} \quad (5)$$

$$\begin{cases} U_{\text{BCGF}} - U_{\text{ADHE}} = U_B - U_A = U_B, V_{\text{BCGF}} - V_{\text{ADHE}} = 0, W_{\text{BCGF}} - W_{\text{ADHE}} = 0 \\ W_{\text{EFGH}} - W_{\text{ABCD}} = W_E - W_A = W_E, U_{\text{EFGH}} - U_{\text{ABCD}} = 0, V_{\text{EFGH}} - V_{\text{ABCD}} = 0 \\ U_A = V_A = W_A = 0, W_B = U_D = V_E = 0 \end{cases} \quad (6)$$

Table 2 presents the mechanical properties of the fiber and resin matrix. The TDE86 resin matrix is assumed to be an elastic-perfectly-plastic material. The fracture energy of the fiber bundles is listed in Table 3.

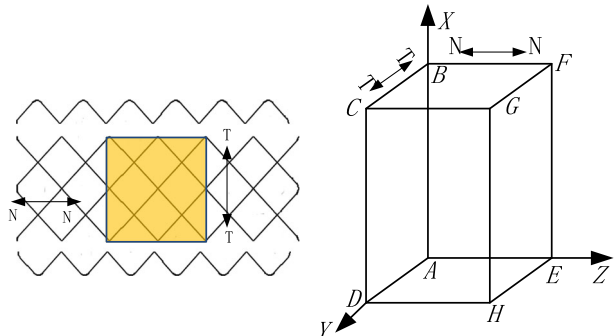Fig. 7 The cutting direction and solid geometry

Table 2 Mechanical properties of the fiber and resin matrix

	E_{11} (GPa)	E_{22} (GPa)	v_{12}	G_{12} (GPa)	G_{23} (GPa)	σ^t (MPa)	σ^c (MPa)	G_f (N/mm)	G_m (N/mm)
T700	230	40	0.26	24	14.3	4900	2470	8	
Matrix	3.5		0.35			80	241		1.5

4 Damage Model

4.1 Progressive Damage Models for the Fiber Yarns

The yarns in the 3D braided composites are assumed to be transversely isotropic. Each yarn under tensile contains one or more damage modes such as tensile, compressive and shear failures in longitudinal and transverse directions. In this paper the initial failure criteria of yarns is the three-dimensional Hashin [27] failure criterion.

Once the damage initiation criteria is satisfied, further loading will cause degradation of the mechanical property which plays an important role in the damage evolvement. In order to realize accurate simulation of the material soften behavior after initial damage appears, an improved damage evolvement model proposed by Fang [11] is adopted instead of traditional direct stiffness reduction model. The evolution law of the damage variable in the post-damage initiation phase is based on the fracture energy dissipated. To alleviate mesh dependency during material softening, a characteristic length of element is introduced into the simulation. The element dissipated energy is expressed as:

$$G_I = \frac{1}{2}\sigma_{eq}^f \varepsilon_{eq}^f l_c \tag{7}$$

Where l_c is a characteristic length of the element and G_I is the fracture energy which is a material property that must be specified. σ_{eq}^f and ε_{eq}^f is the equivalent failure stress and strain respectively.

The reduction of the stiffness coefficients is controlled by damage variables D that might vary from zero (undamaged state) to one (fully damage state). As a result, the macroscopic failure process of materials is a monotone decreasing function about damage variable D. For fiber bundles, take the damage variable of different damage models into constitutive equations of fiber bundles to achieve the stiffness reduction. The energy hypothesis advanced by Cordebos-Sidoroff [28] is implemented to draw damage variables into stiffness matrix as follow:

$$C(d) = C(D) = M^{-1}(D) : C_0 : M^{T,-1}(D) \tag{8}$$

Where C_0 and $C(d)$ are the stiffness tensors for the undamaged and damaged configurations respectively.

Table 3 Fracture energy of fiber reinforced-epoxy composites

G_{Lt} (N/mm)	G_{Lc} (N/mm)	G_{Tt} (N/mm)	G_{Tc} (N/mm)	G_{mt} (N/mm)	G_{mc} (N/mm)
8.0	8.0	1.5	1.5	1.0	1.0

4.2 Cohesive Zone Model

To investigate the interfaces damage mechanism in the RVC model, the CZM described by traction–separation law is established. The initial traction-separation law can be written as:

$$t = \left\{ \begin{array}{c} t_n \\ t_t \\ t_s \end{array} \right\} = \left\{ \begin{array}{ccc} K_{nn} & & \\ & K_{tt} & \\ & & K_{ss} \end{array} \right\} \left\{ \begin{array}{c} \delta_n \\ \delta_t \\ \delta_s \end{array} \right\} \tag{9}$$

Here t_n, t_s and t_t are the stress components in the normal, first and second shear direction, δ_n, δ_s and δ_t represent the displacement components in the normal, first and second shear direction. K_{nn}, K_{ss}, K_{tt} are the stiffness coefficient of interface respectively. Interface damage is assumed to be initial when the quadratic interaction function involving the nominal stress ratios reaches a value of one. The criterion can be represented as:

$$\left\{ \frac{\langle t_n \rangle}{N} \right\}^2 + \left\{ \frac{t_s}{S} \right\}^2 + \left\{ \frac{t_t}{S} \right\}^2 \geq 1 \tag{10}$$

N and S are normal and shear strength of interface. A scalar damage variable d is used to represent the extent of damage in the interface. It initially has a value of 0, and the mechanical properties are linear. It monotonically evolves from 0 to 1 upon further loading. Damage stiffness matrix can be derived as the following equation:

$$K(d) = \begin{bmatrix} (1-d)K_{nn} & & \\ & (1-d)K_{tt} & \\ & & (1-d)K_{ss} \end{bmatrix} \tag{11}$$

The damage variable d is computed from:

$$d = \max \left\{ 0, \min \left\{ 1, \delta_c^f \frac{\delta_c^{eq} - \delta_c^i}{\delta_c^{eq} \left(\delta_c^f - \delta_c^i \right)} \right\} \right\} \tag{12}$$

δ_c^i 和 δ_c^f are the equivalence displacements corresponding to initial damage and final failure. In this work, damage evolution and extension are based on the theory of fracture energy theory. The fracture energy is equal to the area under the traction-separation curve as shown in Fig. 8.

Fig. 8 The traction-separation law of damage of interface element
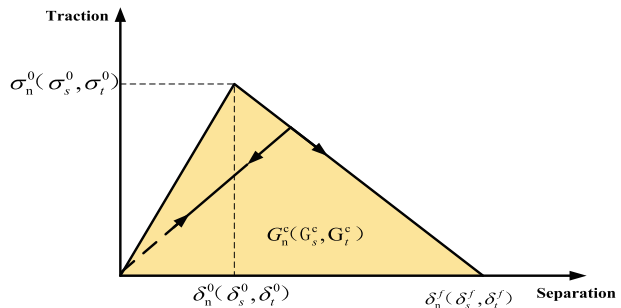
4.3 Matrix Model

The Von-Mises failure criterion is chosen to predict the damage of the isotropic resin matrix noting that the epoxy matrix material is no longer isotropic once the matrix failure occurs. The matrix is assumed to be an elastic-perfectly-plastic material.

$$(\sigma_1 - \sigma_2)^2 + (\sigma_1 - \sigma_3)^2 + (\sigma_3 - \sigma_2)^2 + 6\left(\tau_{12}^2 + \tau_{23}^2 + \tau_{31}^2\right) = 2\sigma_M^2 \tag{13}$$

The damage initiation criterion of matrix within the braided composites can adopt the maximum principle stress criterion which can be expressed as:

$$F_M = \left(\frac{\sigma_{\max}}{X_M^t}\right)^2 \geq 1 \tag{14}$$

For the undamaged elements of matrix, damage factor equals 0. the stiffness of matrix element drops to zero after plastic failure happens.

In order to conduct failure analysis based on an element-by-element scheme, the constitutive equations formulated, the failure criteria, and the degradation model were implemented by using the user-defined material subroutine (UMAT) of ABAQUS in FORTRAN code. UMAT allows material properties to be a direct function of predefined state variables, which themselves can be defined as a function of any quantity at each material integration point such as stress and strain.

5 Results and Discussion

5.1 Simulation Results

The simulation results are compared with experiment data in Table 4. The biggest deviation of the simulation results and experimental result is within 15 %, so the microscomic simulation method of 3D braided composites is reasonable. Here EXP and SIM represent the results of experiment and simulation. For 3D4dC braided composites with one interior cell along thickness direction, there are approximately 20 % reduction in tensile modulus and 60 % reduction in tensile strength compared with the specimens without cut-edge for small braiding angel, while 30 % and 75 % for large braiding angel. It can be discoverable that cut-edge effect is more serious for 3D4d braided composites with larger braiding angle than the ones with smaller braiding angle, so we can appropriately dilute the influence of cut-edge via minishing braiding angle.

Table 4 The comparison of the results of simulation and experiment

	Tensile modulus(GPa)			Tensile strength(MPa)		
	EXP	SIM	Relative errors(%)	EXP	SIM	Relative errors(%)
3D4dU-20	98.6	92.7	5.9 %	1156.2	1010.86	12.5 %
3D4dC-20	78.5	72.6	7.5 %	409.75	373.4	8.8 %
3D4dU-40	39.5	40.96	3.7 %	673.5	621.5	7.7 %
3D4dC-40	27.9	27.44	1.6 %	149.7	156.3	4.4 %

Fig. 9 The tensile stress–strain curves of 3D4d braided composites with $\gamma = 20°$
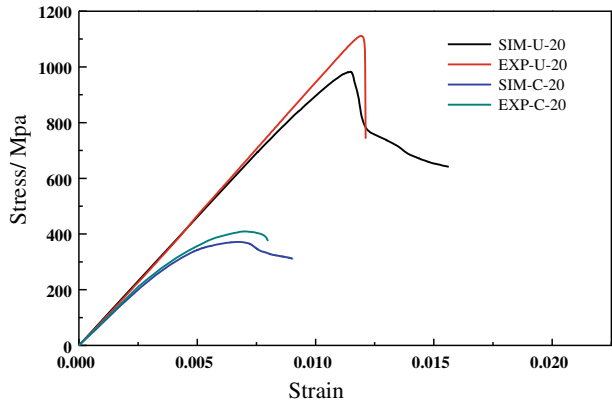
5.2 The Tensile Stress–Strain Curves

As elaborated in section 3, there are different failure modes for braiding yarns, interface and resin matrix. The multiple damage modes might be emerged simultaneously as long as the corresponding failure criteria are satisfied with the increasing tensile stress. The tensile stress–strain curves of 3D4dU and 3D4dC braided composites in comparison with the experimental and numerical results are illustrated in Fig. 9 and Fig. 10. The stress-strain curve of specimens without cut-edge shows linear increase before the initiation damage occurs. The slope of curves and maximum stress of the simulation results are lower than the experimental data which can be attributed to only choose the interior structures but not consider the surface structures. For 3D4dU braided composites, as initial damage occurs, fracture characteristics presents brittle and the stress drops quickly with the increase of strain. The stress-strain curve of the specimens with cut-edge exhibits nonlinear in a short strain range before damage occurs. The initial elastic modulus and ultimate stress decrease with the increase of braiding angle, which is mainly due to tilt level relative to the longitudinal direction of braiding yarns is more inclined for the ones with larger braiding angel. The predicted curves are in good agreement with the experiment data in the linear period of the curves.

The stress–strain curves of 3D4dU and 3D4dC braided composites in comparison with numerical results are illustrated in Fig. 11 and Fig. 12. The initial damage of resin, interface and yarns including longitudinal and transverse damage are marked in stress–strain curves.

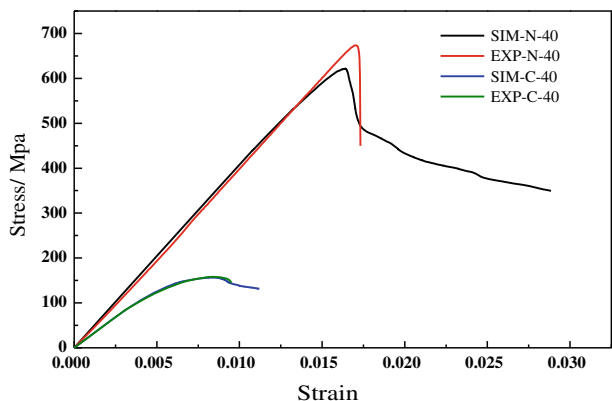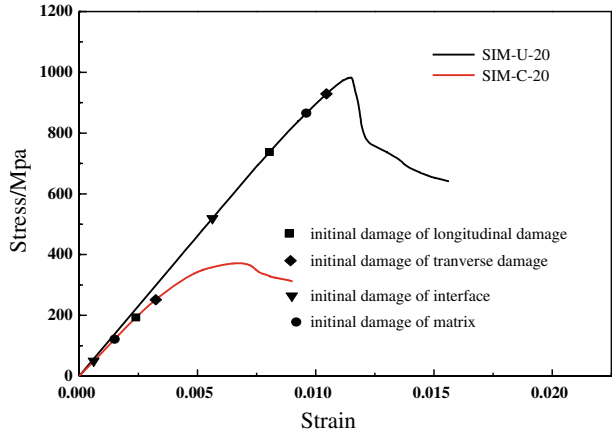**Fig. 10** The tensile stress–strain curves of 3D4d braided composites with $\gamma = 40°$

Fig. 11 The tensile stress–strain curves of simulation with $\gamma = 20°$


Transverse damage for large braiding angel is more serious and appears nearly at the same time with longitudinal damage in Fig. 12. Relative to the initial damage of 3D4dU composite, since cutting effect led to the reductions of the interface mechanical performance, the interface damage occurs even if strain value is relativey very small. Fiber extractions are found in the cutting face of the specimen which is consistent with the experimental phenomenon.

5.3 Evolution of Damage

The damage evolution of the constituents is important for the numerical results. Damage evolution analysis have a thorough understanding of material failure mechanism and the regularity of damage evolution for each component, especially this part of the research in the condition of cut-edge is very scarce. In addition, Fig. 13 shows the damage evolution of 3D4dU braided composites when the braiding angel is40°. The damage initiation of interface occurs at $\varepsilon = 0.48\%$,the mechanical property almost has not been affected and the curve remains linear for the initial damage is local and little. When $\varepsilon = 1.29\%$,the longitudinal and transverse damage appear in the stress concentration zones where braiding yarns and resin matrix contact. Resin matrix do not yield and the damage factor of interface is less than 0.3 contributing little

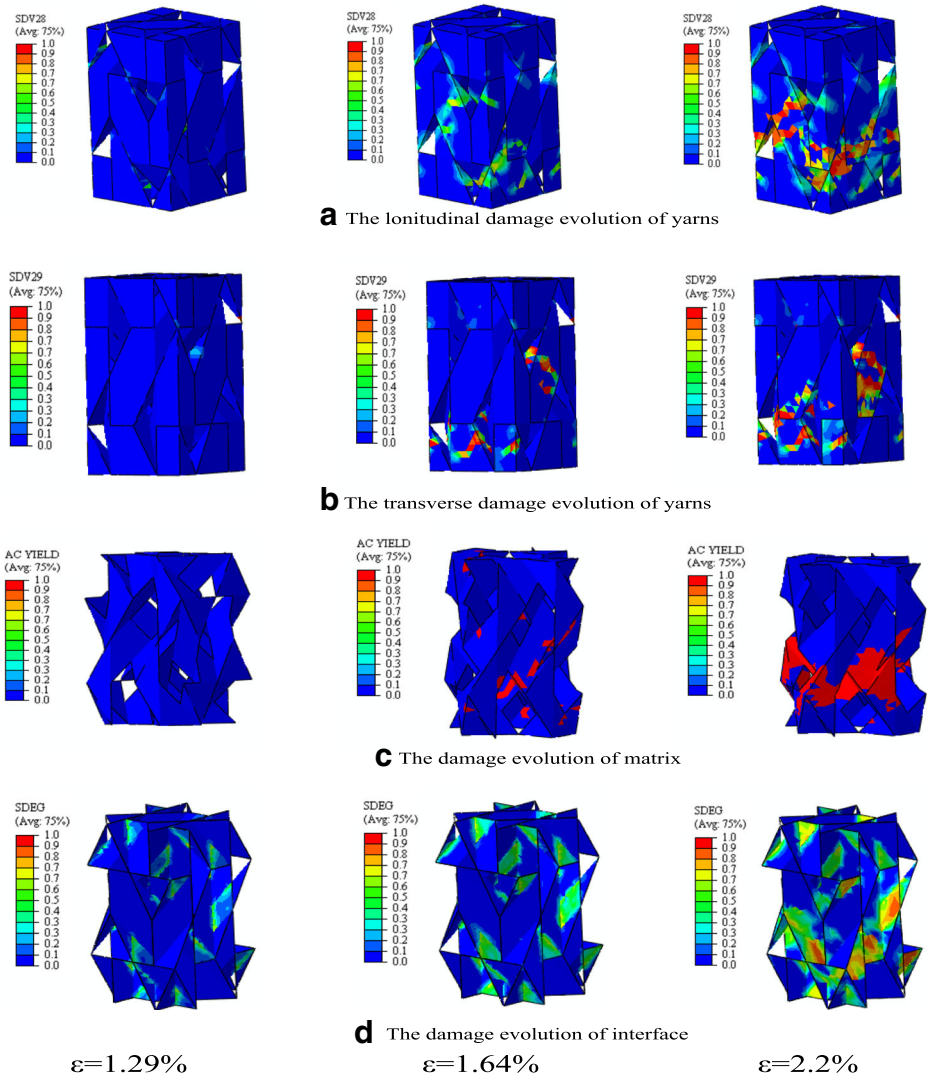**Fig. 12** The tensile stress–strain curves of simulation with $\gamma = 40°$

a The lonitudinal damage evolution of yarns

b The transverse damage evolution of yarns

c The damage evolution of matrix

d The damage evolution of interface

$\varepsilon=1.29\%$ $\varepsilon=1.64\%$ $\varepsilon=2.2\%$
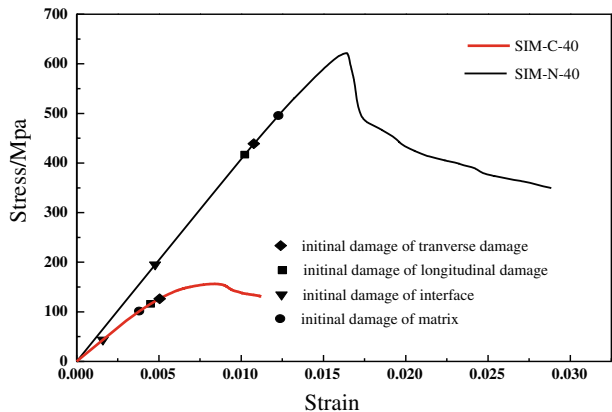
Fig. 13 The propagation of 3D4dU braided composites with $\gamma=40°$

influence on the mechanical property. When $\varepsilon=1.64\%$(the stress peak of the 3D4dU curve in Fig. 12), the longitudinal and transverse damage extend from contacting region to surrounding region, part of elements are completely destructive at the same time the stress drops quickly with the increase of strain. For the yield behaviour of resin, its plasticity occurs at $\varepsilon=1.31\%$. When $\varepsilon=2.2\%$,the degree of longitudinal and transverse damage of yarns reaches extreme, a large area of resin and interface are destructive in the RVE model. There are longitudinal tensile-shear and transverse shear failure. Some yarns are pulled out so there exists the phenomenon of interface debonding, and the results of simulation and experiment are consistent in agreement.

Figure 14 shows the damage evolution of 3D4dC braided composites with $\gamma=40°$, the initial damage emerges in the interface near the cutting face at $\varepsilon=0.16\%$. As the strain comes to 0.6 %, the interface damage area expands from the cut face into interior part and the
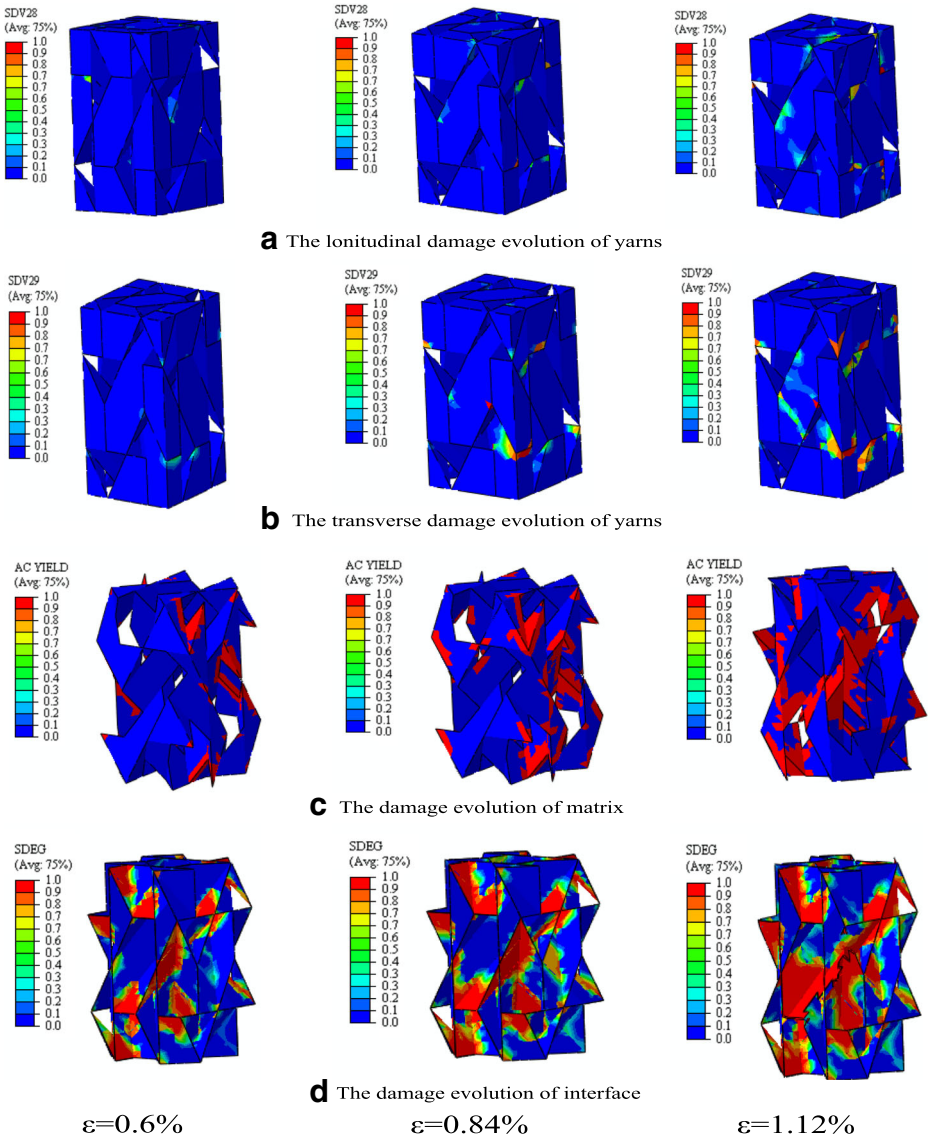
a The lonitudinal damage evolution of yarns

b The transverse damage evolution of yarns

c The damage evolution of matrix

d The damage evolution of interface

ε=0.6%   ε=0.84%   ε=1.12%

Fig. 14 The propagation of 3D4dC braided composites with $\gamma = 40°$

transverse damage of yarns emerges in the zones where the yarns interlace each other. The yielding of the resin matrix occurs near the cutting face. The slope of the curve begins to drop slowly at $\varepsilon = 0.84\%$(stress peak of 3D4dC curve in Fig. 12). The curve remains nonlinear and the slope descends more rapidly than before because the destruction of interface weaken bonding performances between braiding yarns under longitudinal tensile. At the peak stress point, the damage area of braiding yarns is small and concentrated in the contact region. The extent of interfaces damage between the yarns are too seriously to bear load at $\varepsilon = 1.12\%$. 3D4dC braided composites cannot bear load continuously due to the fiber pulling-out and interfaces debonding.

6 The Variation of Cut-Edge Effect with Thickness

By comparing the simulation and experimental results we have verified the rationality of the progressive damage analysis on the cut-edge effect in section 5. When the thickness of the specimens corresponding to the number interior cells along thickness direction increase,it inevitably will be another cut-edge effect. Experimental researches of each kind of specimen will augment the cost and time, so it is significant to study the variation of cut-edge effect with thickness through simulation method. Stack the RVCs together and exert the periodic boundary condition of cut-edge state on RVCs. Here consider the braiding angle of 40°as the analysis object and n as the number of interior cells. As stacking one more inner cell, the thickness adds to 1.9 mm. For example, when $n = 4$, the thickness of 3D4dU braided composites with braiding angel 40°is 9.2 mm.

Figure 15 shows the stress-strain curves of uncut-edge condition and cut-edge conditions of different numbers of interior cells. With the increase of the thickness, the slope and maximum stress of the curve largen, that stiffness and strength continuously strengthen. Cut-edge influence on the mechanical properties of 3D4d braided composites is weakening with the increase of thickness. The stress-strain curves of 3D4dC-5 and 3D4dC-10 nearly overlap meaning there exists an upper limit of cut-edge effect with the increase of thickness.

Figure 16 shows the tensile stiffness and strength values of different numbers of internal cell. There are approximately 9.3 % reduction in tensile modulus and 17.6 % reduction in the tensile strength when n greater than or equal five.

When n equals one in Section 5, the debonding of interface and pulling out of yarns lead to the failure of 3D4dC braided composites. While the thickness of the specimen increases, the cut-edge on the surface may only has influence on the near surface area and less influence on internal structure. Internal braiding yarns are the main load bearing. Figure 17 shows the interface propagation of 3D4dC-4 braided composites. The initial damage emerges near the cutting face at $\varepsilon = 0.35\%$ and expands from the cut face into interior part. The cut portion and surrounding portion of the interface just completely destroyed when materials forfeit bearring capacity at $\varepsilon = 1.3\%$, internal interface although appears imparity degrees of damage, but the damage factors are relatively small. It is visible that the increase in the thickness enhance the overall interface properties and the mechanical properties of 3D4d braided composites.

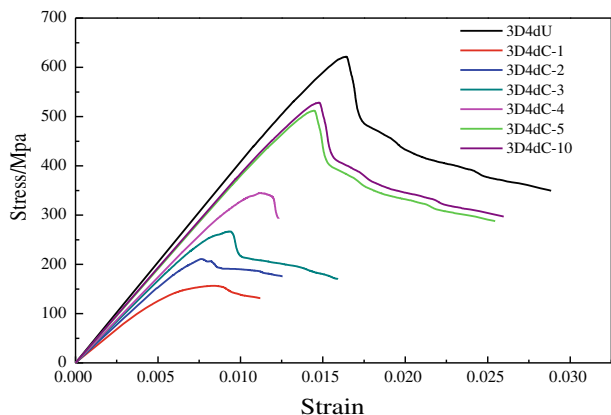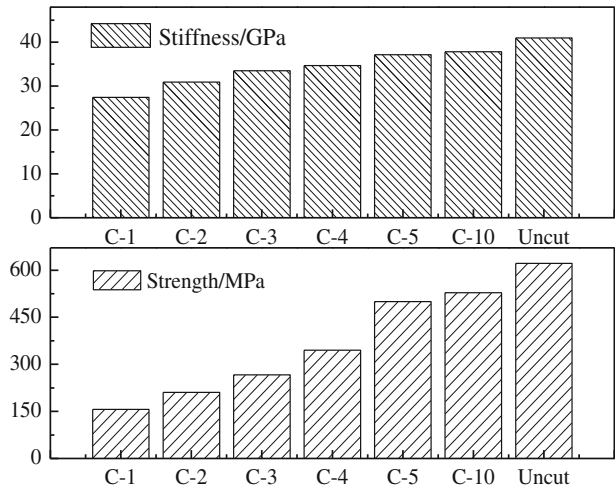Fig. 15 The variation of cut-edge effect with thickness

Fig. 16 Tensile stiffness and strength values of different numbers of internal cell

7 Conclusions

In this paper, the cut-edge effect on uniaxial tensile property of the 3D4d braided composites with different braiding angels is studied by experiment and simulation method. This paper adopts a new kind of periodic boundary condition to simulate the cut-edge and verifies rationality of the simulation analysis method, finally discuss the variation of cut-edge effect with thickness through superimposing inner cells. The goal of simulation of cut-edge effect is weakening the cut-edge influence on material mechanics as much as possible in actual engineering application.

(1)   Cut-edge has a great influence on the longitudinal strength for thin 3D4d braided composites along thickness direction. The fracture of yarns, debonding of interface and pulling out of yarns lead to the failure of 3D4dC braided composites when subjected tensile;
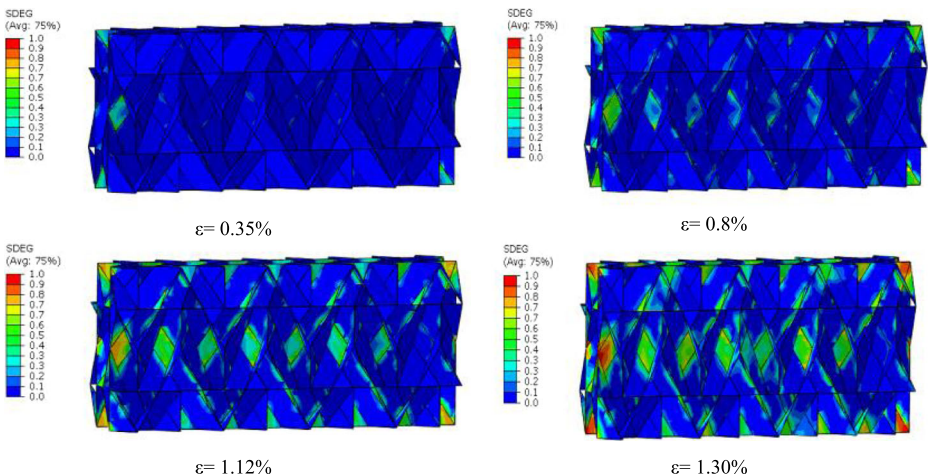

$\varepsilon = 0.35\%$

$\varepsilon = 0.8\%$

$\varepsilon = 1.12\%$

$\varepsilon = 1.30\%$

Fig. 17 The interface propagation of 3D4dC-4 braided composite

(2)   The damage propagation of a representative volume cell (RVC) is analyzed by using a damage model in finite element method to evaluate the non-linear behavior of the 3D4d braided composites. To investigate the interfaces debonding, the cohesive zone model described by traction-separation law is established. Two different periodic boundary conditions are applied for cue-edge and uncut-edge conditions. Stress-strain distribution and the damage evolution nephogram in cut-edge conditions were conducted by simulation analysis method.

(3)   The variation of cut-edge effect with thickness was studied through simulation method. Cut-edge influence on the mechanical properties of 3D4d braided composites is weakening with the increase of thickness. That is when the numbers of interior cells of 3D4d braided composites is greater than or equal to five, the mechanical properties of cut-edge condition in this paper come to a head.

References

1. Liu Z.G.: Study on comparison of manufacturing methods of high performance composites pipes and application of 3D braiding technology. J. Mater. Eng. **2**, 109–111 (2009)
2. Tang Z.X., Postle R.: Mechanics of three-dimensional braided structures for composite materialsII:prediction of the elastic modulus. Compos. Struct. **54**, 451–457 (2001)
3. Shokrieh M., Mazloomi M.: A new analytical model for calculation of stiffness of three-dimensional four directional braided composites. Compos. Struct. **94**, 1005–1015 (2012)
4. Sun H.Y., Qiao X.: Prediction of the mechanical properties of 3-dimensional braided composites. Compos. Sci. Technol. **57**, 623–629 (1997)
5. Ishikawa T., Chou T.W.: Stiffness and strength behavior of woven fabric composites. J. Mater. Sci. **17**, 3211–3220 (1982)
6. Kalidindi S.R., Abusafieh A.: Longitudinal and transverse moduli and strengths of low angle 3-D braided composites. J. Compos. Mater. **30**, 885–905 (1996)
7. Macander AB, Crane RM, Camponeschi ET. Fabrication and mechnical properties multidimensionally (X-D) braided composite materials. Composite materials: Testing and design (7th conference). [C] STP. p. 422–43 (1986)
8. Li J L., Jiao Y N., Y. S.: Experimental investigation of cut-edge effect on mechanical properties of three-dimensional braided composites. Materials and Design. **28**, 2417–2424 (2007)
9. Zhang C., Binienda W.K.: Free-edge effect on the effective stiffness of single-layer triaxially braided composite. Compos. Sci. Technol. **107**, 145–153 (2015)
10. Li D.S., Fang D.N., Jiang N., et al.: Finite element modeling of mechanical properties of 3D five-directional rectangular braided composites. Compos Part B ENG. **42**, 1373–1385 (2011)
11. Zhang C., Xu X.: W, finite element analysis of 3D braided composites based on three unit-cells models. Compos. Struct. **98**, 130–142 (2013)
12. Fang G.D., Liang J., Wang B.L.: Progressive damage and nonlinear analysis of 3D four-directional braided composites under unidirectional tension. Compos. Struct. **89**, 126–133 (2009)
13. Zeng T., Fang D.: N, predicting the nonlinear response and failure of 3D braided composites. Mater. Lett. **58**, 3237–3241 (2004)
14. Hu L. Investigation on progressive damage and failure mechanism of three dimensional braided composites [D]. Dissertation, Beihang University, 55–65 (2015)
15. Wang Y.Q., Wang A.S.D.: Spatial distribution of yarns and mechanical properties in 3D braided tubular composites. Appl. Compos. Mater. **4**, 121–132 (1997)
16. Li D.S., Fang D.N., Lu Z.X., Yang Z.Y., Jiang N.: Finite element analysis of mechanical properties of 3D four directional rectangular braided composites part 2:validation of 3D finite element model. Appl. Compos. Mater. **7**, 389–404 (2010)
17. Xia B., Yang Z Y.: Investigation on the tensile properties of three-dimensional full five-directional braided composites. Comp Mater Sci. **77**, 445–455 (2013)
18. Li D.S., Li J.L.: Chen Li.Finite Element analysis of mechanical properties of 3D four-directional rectangular braided composites. Appl. Compos. Mater. **17**, 373–387 (2010)

19. Xu K.: Xu X W. Finite element analysis of mechanical properties of 3D five-directional braided composites. Mat Sci ENG A-Struct. **487**, 499–509 (2008)
20. Sun H., CC W.: Experimental research on mechanical properties of composite materials with textile structure. J Exp Mech. **012**, 335–341 (1997)
21. Zhao Q., Jin L., Jiang L., Zhang Y., Sun B.: Experimental characterizations of bending fatigue of a four-step 3-D braided rectangular composite under different stress levels. J. Reinf. Plast. Compos. **30**(1571–1582), (2011)
22. Rawal A., Sibal A., Saraswat H.: Tensile behaviour of regular triaxial braided structures. Mech. Mater. **91**(277–289), (2015)
23. D'Amato E.: Experiments on single layer textile composites. Compos. Struct. **55**(217–223), (2002)
24. Xie D., Biggers S B.: Calculation of transient strain energy release rates under impact loading based on the virtual crack closure technique. Impact Eng. **34**, 1047–1060 (2007)
25. Fang G.D., Liang J.: Effect of interface properties on mechanical behavior of 3D four-directional braided composites with large braid angle subjected to uniaxial tension. Appl. Compos. Mater. **18**, 449–465 (2011)
26. Shriram S., Pagano N J., Somnath G.: Analysis of interfacial debonding in three-dimensional composite microstructures. J ENG MATER-T ASME. **128**, 96–106 (2005)
27. Hashin Z.: Failure criteria for unidirectional fiber composites. J. Appl. Mech. **47**, 329–334 (1980)
28. Cordebois J., Sidoroff F.: Damage induced elastic anisotropy, Mechanical behavior of anisotropic solids. Comportment mechanique des Solids Anisotropes. **24**, 761–774 (1982)